A MATHEMATICAL TOOL TO RECOGNIZE IONOSPHERIC TSUNAMI DUE TO TROPICAL CYCLONE: A CASE SUCH AS TYPHOON NAKRI ON 29 MAY 2008

Jyh-Woei, Lin

Department of Electrical Engineering,
Southern Taiwan University of Science and Technology, Tainan City,
TAIWAN.

pgjwl1966@gmail.com

ABSTRACT

In this paper uses, a mathematical tool called two dimensional Principal Component Analysis (2DPCA) to determine total electron content (TEC) anomalies in the ionosphere for a Tropical Cyclone such as the Nakri Typhoon on 29 May, 2008 (UTC). 2DPCA are applied to the global ionospheric TEC data with transforms conducted for the time period 12:00 to 14:00UT on 29 May 2008 when the wind was most intense. Results show that at a height of approximately 150-200 km the TEC anomaly is more localized; however its intensity increases with height and becomes more widespread. The TEC anomaly is akin to an ionospheric tsunami. Potential causes of the results are discussed with emphasis given to vertical acoustic gravity waves. The approximate position of the typhoon's eye can be detected if the TEC data are divided into fine enough maps with adequate spatial-resolution at GPS-TEC receivers. This implies that the trace of the typhoon is caught using 2DPCA.

Keywords: Two Dimensional Principal Component Analysis (2DPCA), Total Electron Content (TEC), Tropical Cyclone, Vertical acoustic gravity waves

INTRODUCTION

A benefit of using GPS satellites in precision geodetic measurement has been the ability to measure Total Electron Content (TEC) in the ionosphere through phase and code measurements of signal delay between receivers and satellites. Furthermore, continued development of dense ground-receiver networks has allowed for 2D and 3D imaging of dynamic changes in ionospheric plasma. One potential area of application is in the study of typhoon related TEC anomalies. Association between typhoon activity and TEC anomalies dates back to the work of Bauer (reference) in the 1950s who noticed that the FoF2 region of the ionosphere would rise and reach maximum height just before the typhoon arrived at the observation station. Other more recent research has also noted fluctuations in the FoF2 layer as typhoons approach (Shen 1982; Liu et al 2006 a & b). Huang et al. (1985) researched 15 typhoons though out 1982 and 1983 near Taiwan using a real-time HF Doppler frequency-shift sounding array to detect ionospheric Doppler frequency shifts (DFS) induced by typhoons. Among their results, two typhoons, Wayne and Andy, caused significant ionospheric variations, which were attributable to typhoon-generated acoustic gravity waves. These could be detected by the sounding system. In a more recent study, Mao et al. (2009) found that anomalous TEC behavior relating to Typhoon Matsa could be distinguished using a GPS-TEC map based on 50 GPS stations covering the IGSGPS tracking network, CMONOC GPS tracking network, and Shanghai GPS tracking network from June 30 to August 19, 2005. Their analysis showed that TEC increased before the landing of Typhoon Matsa, with TEC increasing from its monthly median over the typhoon area by about 5 TEC

Leena and Luna International, Chkusei, Japan.
(株) リナアンドルナインターナショナル, 筑西市,日本
Copyright © 2016

units (1 TECu=10^{16} electrons/m^2). The magnitude and the area of increased-TEC decreased with the landing of the typhoon. One day after the passage of the typhoon, TEC reached a minimum and was lower than its monthly median. Kazimirovsky et al. (2003) provides an excellent review of the state of knowledge as of 2003 on potential causes of ionospheric anomalies from anthropogenic causes through to the weather and other natural phenomena. Explanations as to the cause of typhoon-related TEC anomalies include typhoon-generated acoustic gravity waves and internal gravity waves (IGWs), which are dependent on temperature and wind structure in the atmosphere. Coupling between typhoon processes and the ionosphere has been discussed by many researchers in recent times (Kazimirovsky, 2002; Sun et al., 2007; Xu et al., 2008; Mao et al., 2009; Liu et al. 2010). These studies of TEC anomalies, however, have been based on observational methods such as deviations from running medians, and not pure mathematical analysis.

In theory, the upward propagation of internal atmospheric disturbances such as planetary waves, tides and gravity waves into the troposphere and stratosphere create the momentum necessary to influence the thermosphere/ionosphere (Kazimirovsky et al, 2003). However, there have been few studies demonstrating the coupling between the troposphere and thermosphere/ionosphere. Two researchers Bishop and Straus (2006) investigated more than ten tropical cyclones (TCs) using GPS occultation data to examine the relationship between ionospheric TEC and TCs. The impact on TEC was measured over a horizontal distance of 2000km from the cyclones' centers and the results found that significant scintillation on TEC could be recorded within 1200km of a storm center. Lin (2010a, 2011a) used principal component analysis (PCA) to describe the spatial distribution of earthquake related TEC anomalies to the Sichuan basin, Wenchuan, China M_w =7.9 earthquake of 12 May, 2008. The studies showed the distribution of both a precursor TEC anomaly and a post earthquake anomaly. For the post earthquake anomaly, the study found that at lower altitudes (200km) the TEC anomaly was spread over a wide range and this range declined with height and the anomaly intensified (300km altitude).

The goal of this paper is to use 2DPCA, which is better than PCA to recognize spatial distribution of any typhoon driven ionospheric TEC anomaly associated with Typhoon Nakri on 29 May 2008 (UTC). The time period chosen is 12:00-14:00 on 29 May 2008 when the wind was very intense (Table 1 and Fig.1).

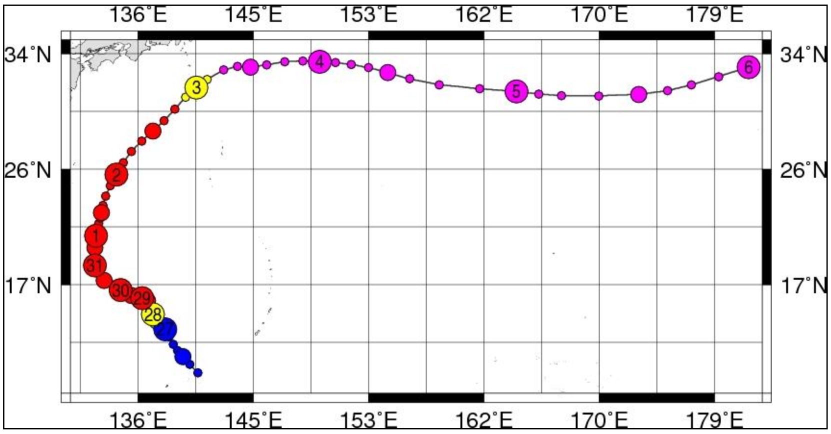

Figure 1. Route of Typhoon Nakri. The time is UTC

Table1. Information about Typhoon Nakri (Japan Meteorological Agency Best Track Data Correction Date: 2008-07-07)

Year	*Month*	*Day*	*Hour*	*Lat.*	*Long.*	*Pressure (hPa)*	*Wind (kt)*
2008	5	26	6	10.5	140.4	1008	0
2008	5	26	12	11.7	139.3	1010	0
2008	5	26	18	12.6	138.6	1008	0
2008	5	27	0	13.7	138.0	1006	0
2008	5	27	6	14.3	137.6	1000	35
2008	5	27	12	14.3	137.4	996	40
2008	5	27	18	14.4	137.2	990	45
2008	5	28	0	14.8	137.1	985	55
2008	5	28	6	15.5	136.8	980	65
2008	5	28	12	15.8	136.7	970	70
2008	5	28	18	16	136.6	955	80
2008	5	29	0	16	136.3	950	85
2008	5	29	6	16.2	135.8	940	95
2008	5	29	12	16.2	135.5	930	**100**
2008	5	29	18	16.4	135.1	930	**100**
2008	5	30	0	16.6	134.7	930	**100**
2008	5	30	6	17	134.1	940	95
2008	5	30	12	17.3	133.5	950	85
2008	5	30	18	17.9	133	960	80
2008	5	31	0	18.4	132.8	965	75
2008	5	31	6	19.2	132.8	970	70
2008	5	31	12	19.7	132.8	970	65
2008	5	31	18	20.2	132.8	970	65
2008	6	1	0	20.6	132.9	970	70
2008	6	1	6	21.5	133.1	970	70
2008	6	1	12	22.3	133.3	970	70
2008	6	1	18	23.5	133.6	965	75
2008	6	2	0	25.1	134.4	960	75
2008	6	2	6	26.8	135.5	960	75
2008	6	2	12	28.3	137.1	965	75
2008	6	2	18	29.9	138.7	970	70
2008	6	2	21	30.8	139.5	975	60
2008	6	3	0	31.5	140.3	980	55
2008	6	3	3	32.1	141.1	985	50
2008	6	3	6	32.8	142.3	990	0
2008	6	3	12	33	144.3	994	0
2008	6	3	18	33.4	146.8	996	0
2008	6	4	0	33.4	149.4	1000	0
2008	6	4	6	33.2	151.7	1004	0
2008	6	4	12	32.6	154.4	1004	0
2008	6	4	18	31.7	158.2	1006	0
2008	6	5	0	31.2	163.9	1008	0
2008	6	5	6	30.9	167.2	1008	0
2008	6	5	12	31	172.9	1008	0
2008	6	5	18	31.7	176.8	1008	0
2008	6	6	0	33	181	1008	0

SOURCE DATA

Data is from the Formosat-3 satellite, updated every 90 min with approximately 2500 profiles daily, and the IGS ground receiver network. Finally a brief discussion of the possible causes and physical meaning of the anomaly as well as the possibility of tracking of a typhoon are given.

Two-Dimensional Component Analysis (2DPCA)

For 2DPCA, let **TEC data** of a region be represented by a matrix *A* (the dimension of *n* x *m*). Linear projection of the form is considered as followed (Sanguansat 2012),

$$y = Ax \qquad (1)$$

Here x is an n dimensional project axis and y is the projected feature of signals on x called principal component vector.

$$S_x = E(y - Ey)(y - Ey)^T \qquad (2)$$

Here S_x is the covariance matrix of the project feature vector.

The trace of S_x is defined;

$$J(x) = tr(S_x) \qquad (3)$$

$tr(S_x) = tr\{x^T Gx\}$, where $G = E[(A - EA)^T (A - EA)]$ (4)

The matrix G is called covariance matrix. The vector x maximizing Eq.4 corresponds to the largest (principal) eigenvalue of G, and let the largest eigenvalue be the most dominant component of the TEC data in this region, therefore largest eigenvalue is represented the principal characteristics or situation of the TEC data in this region. 2DPCA can be removed small sample signal size (SSS) problem. The PCA converts the measurements into one-dimensional data before covariance matrix calculation. The covariance matrix of PCA is based on an input matrix with the dimension of *m x n*, which is reshaped from one-dimensional data (length of m multiplying n). Reshaping data will cause computing error because PCA is a tool to deal with one-dimensional data. It means that the spatial structure and information can not be well preserved due to some original information loss when inverting to original dimension under the condition of the matrix being small sample size (SSS). Such information loss is called SSS problem. However, the covariance matrix in 2DPCA is full rank for a matrix of low dimension. Therefore the curse of dimensionality and SSS problem can be avoided. TEC data are examined to detect Xiaolin mudslide-related TEC anomaly and GIMs are only used to observe TEC situation in this study.

DATA PROCESSING AND RESULTS

Figure 2(a) shows the GIM on 29 May for 12:00-14:00UT. Figure 2(b) gives a color-coded scale of the magnitudes of principal eigenvalues corresponding to Fig. 2(a). Color intensity denotes magnitude. From the figure it can be seen that 100 principal eigenvalues are assigned (i.e., each grid in the bottom figures represents a principal eigenvalue). Figures 3-7 show the same approach but for different heights. Varying color intensity, representative of large principal eigenvalues in the bottom figures of Figs. 2 to 7, shows the existence of a TEC anomaly, much like an ionospheric tsunami, over the region of the position of Typhoon Nakri at 16.2°N, 135.5°E (Table 1) The anomaly becomes more widespread with height. At 150 to 200 m it is intense and highly localized. With height the anomaly remains intense in the same localized region but also shows to be more widespread around this intense center (Fig. 2-7).

Copyright © 2016

Leena and Luna International, Chikusei, Japan.
(株) リナアンドルナインターナショナル, 筑西市,日本
ISSN: 2186-8476, ISSN: 2186-8468 Print
www.ajsc. leena-luna.co.jp

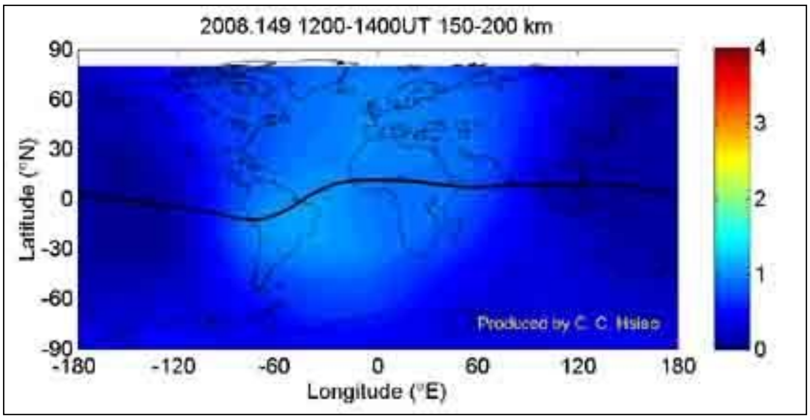

Figure 2a. GIM on 29 May at height 150-200 km for the time period 12:00-14:00UT.

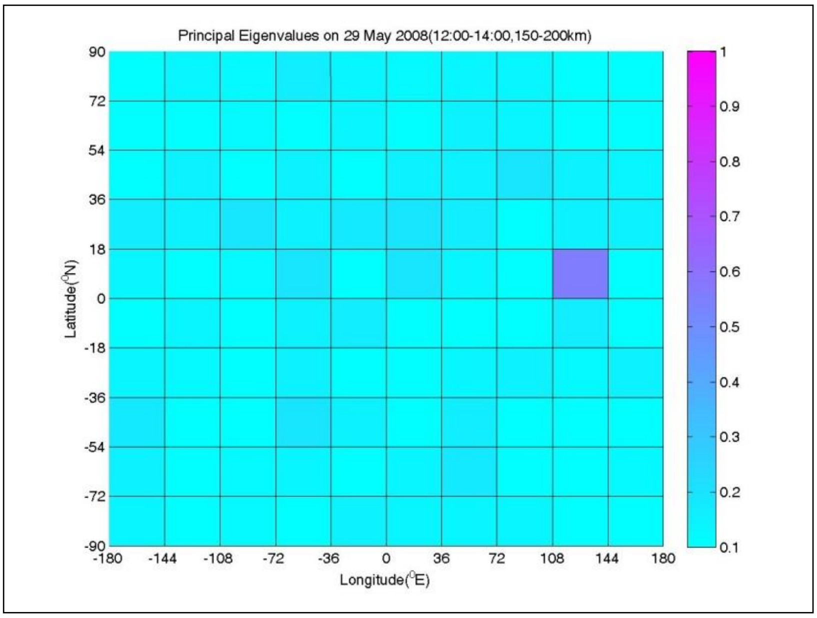

Figure 2b. Color-coded scale of the magnitudes of principal eigenvalues corresponding to Fig. 2a. The color within a grid denotes the magnitude of a principal eigenvalue corresponding to Fig. 2a, so that there are 100 principal eigenvalues assigned (i.e., each grid in the bottom figures represents a principal eigenvalue), respectively.

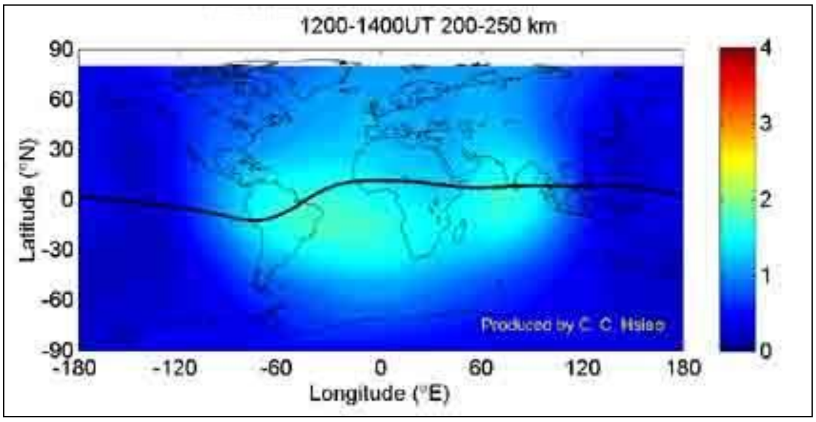

Figure 3a. GIM on 29 May at height 200-250 km for time 12:00-14:00UT.

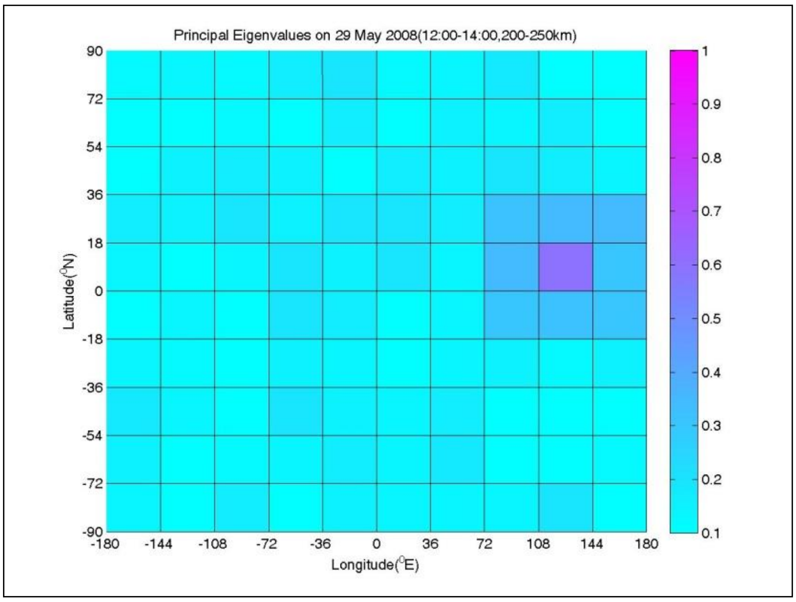

Figure 3b. Color-coded scale of the magnitudes of principal eigenvalues related to Fig. 3a.

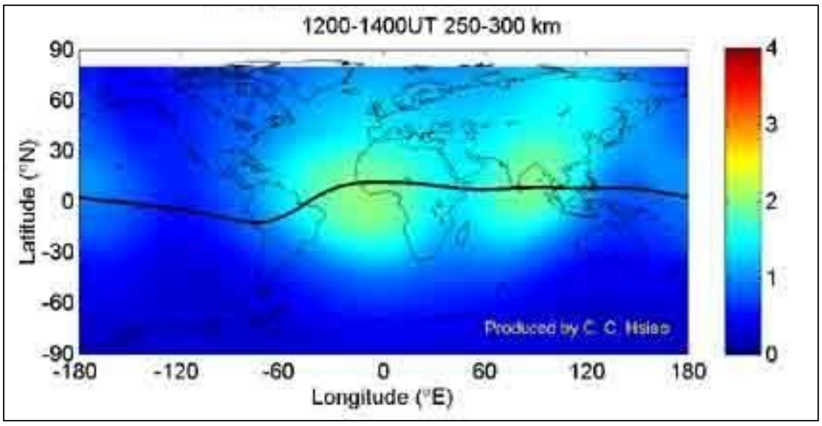

Figure 4a. GIM on 29 May at height 250-300 km for time 12:00-14:00UT.

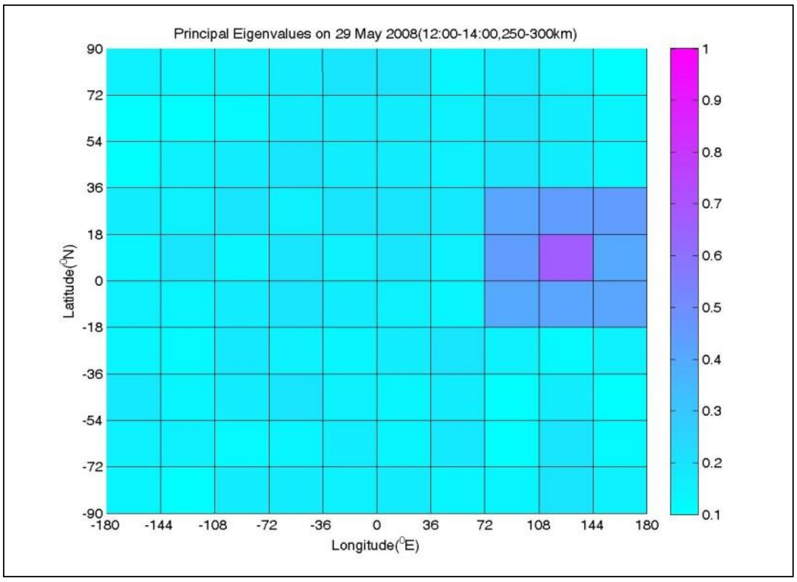

Figure 4b. Color-coded scale of the magnitudes of principal eigenvalues related to Fig. 4a.

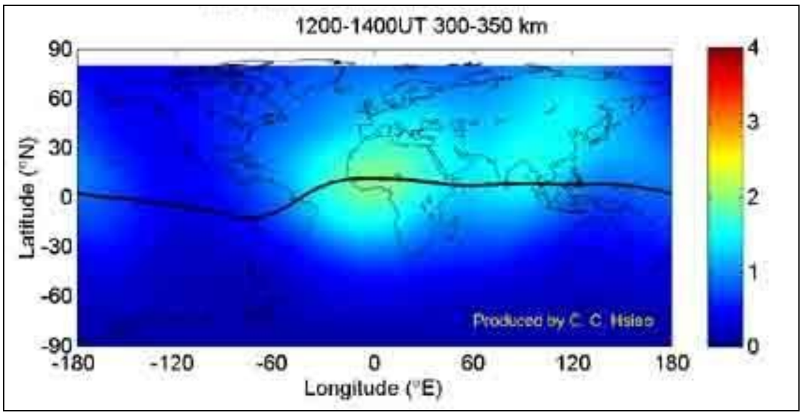

Figure 5a. GIM on 29 May at height 300-350 km for time 12:00-14:00UT.

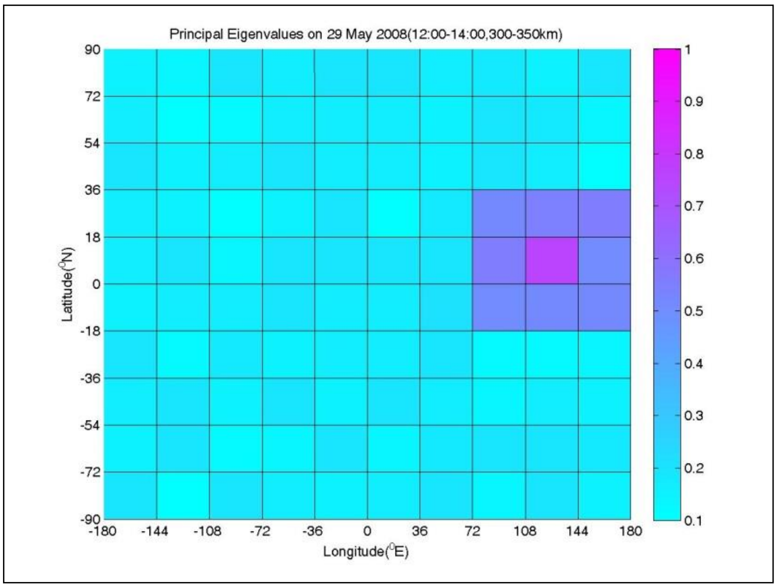

Figure 5b. Color-coded scale of the magnitudes of principal eigenvalues related to Fig. 5a.

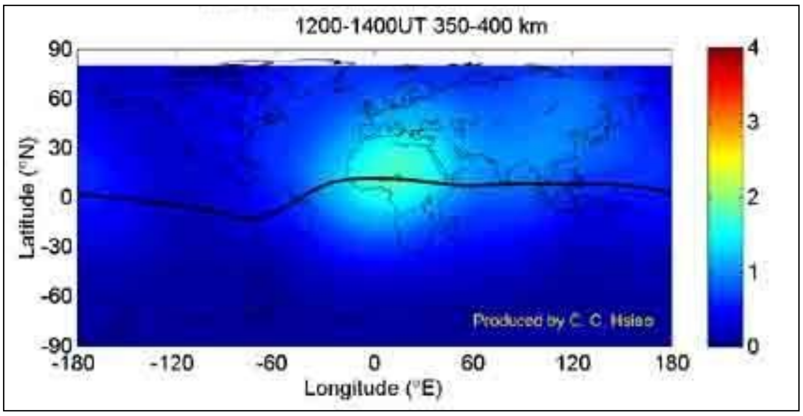

Figure 6a. GIM on 29 May at height 350-400 km for time 12:00-14:00UT.

ISSN: 2186-8476, ISSN: 2186-8468 Print
www.ajsc.leena-luna.co.jp
Leena and Luna International, Chkusei, Japan.
(株) リナアンドルナインターナショナル, 筑西市,日本
Copyright © 2016

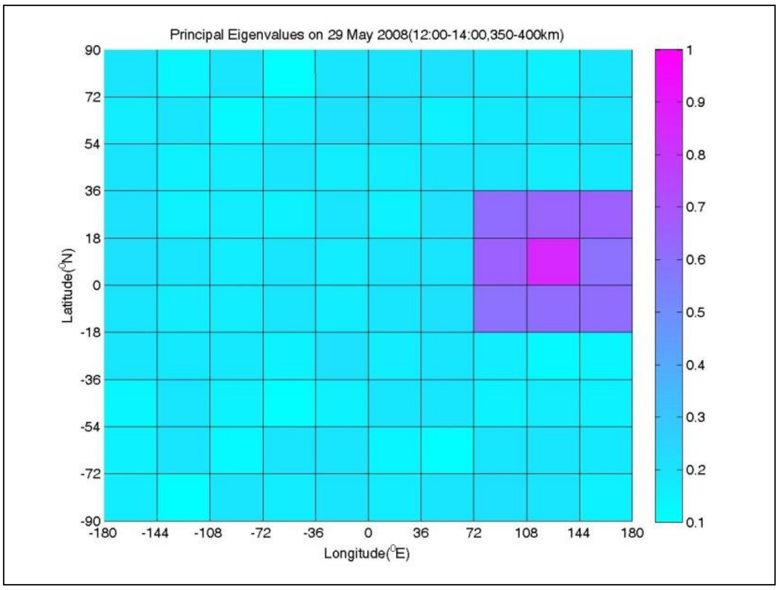

Figure 6b. Color-coded scale of the magnitudes of principal eigenvalues related to Fig. 6a.

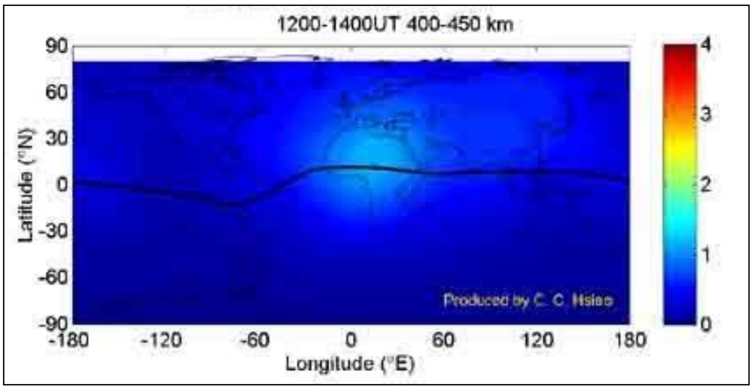

Figure 7a. GIM on 29 May at height 400-450 km at 12:00-18:00 UT.

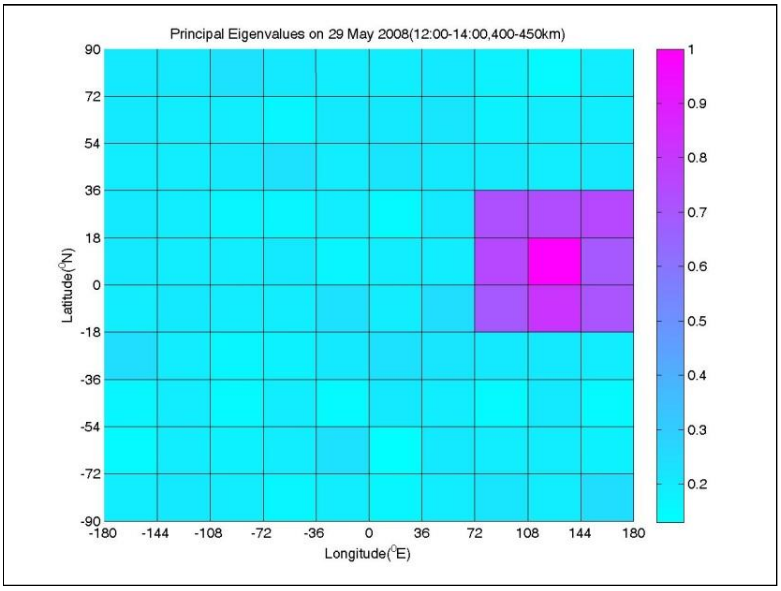

Figure 7b. Color-coded scale of the magnitudes of principal eigenvalues related to Fig. 7a.

Leena and Luna International, Chikusei, Japan.
(株) リナアンドルナインターナショナル, 筑西市,日本
ISSN: 2186-8476, ISSN: 2186-8468 Print
www.ajsc. leena-luna.co.jp

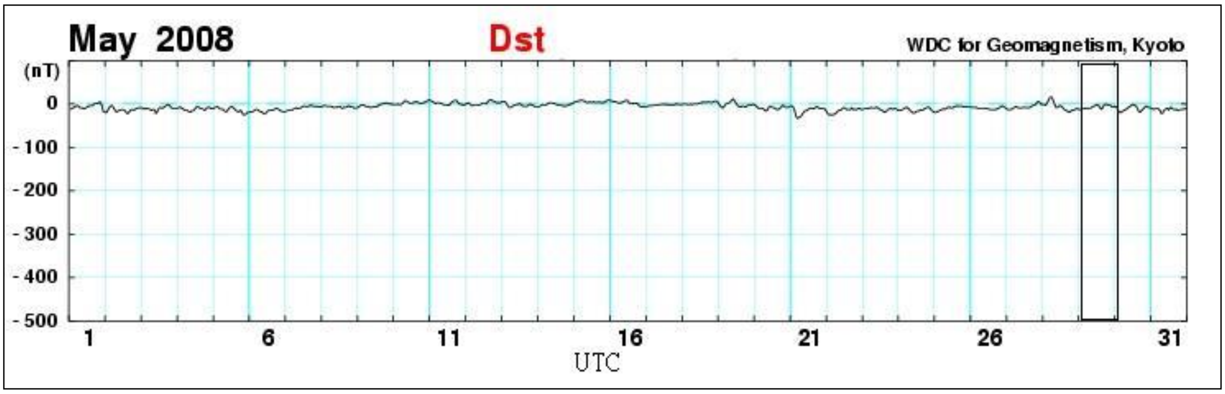

Figure 8a. Dst indices in May 2008 (World Data Center for Geomagnetism, Kyoto). The DST indices on 29 May are within the rectangle

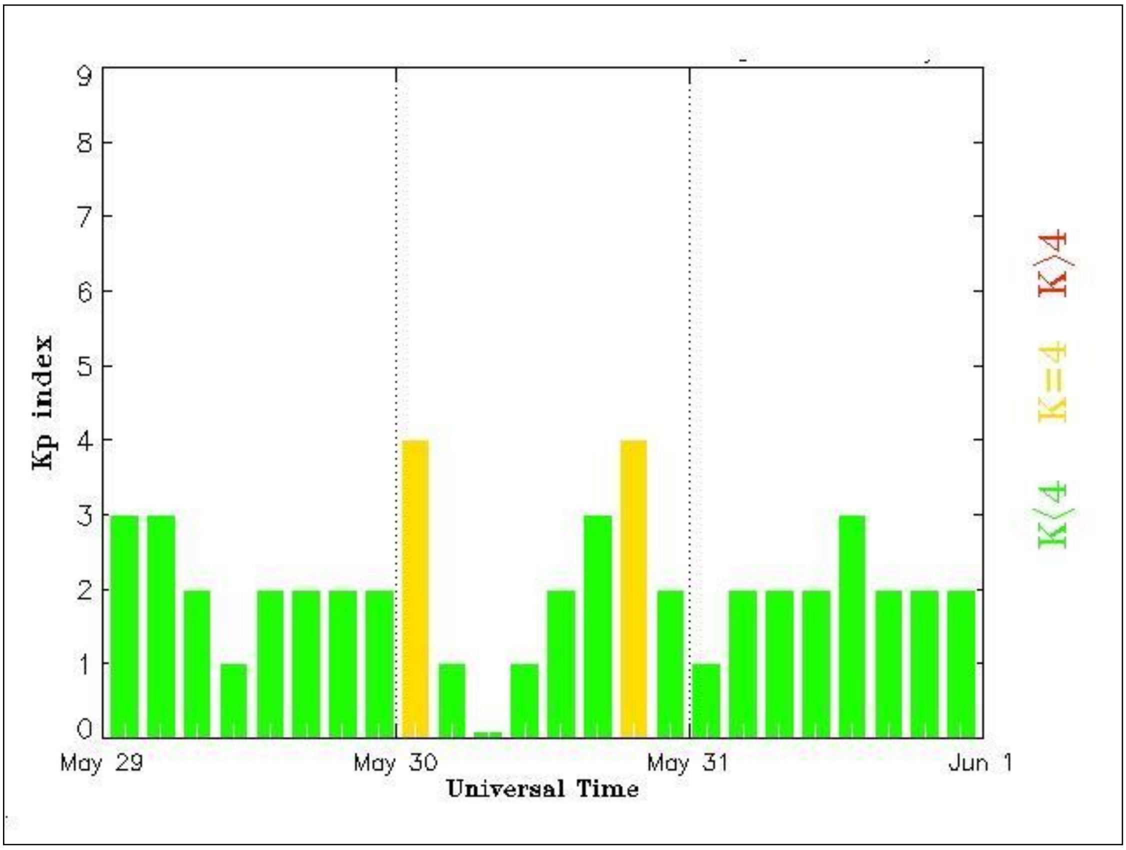

Figure 8b. Kp indices from 29 to 31 May 2008 (NOAA Space Center).

The possibility of other factors such a solar flare and geomagnetic effects affecting the results are considered by examining the Dst indices and Kp indices (Elsner and Kavlakov, 2001; Mukherjee, 1999; Hamilton et al., 1986) in Figs. 8a and b, respectively. Figure 8a shows that for May the Dst index was relatively flat indicating that geomagnetic storm activity could not have been responsible for the TEC anomaly. Similar to Fig. 8a, Fig. 8b shows that geomagnetic storm activity was low during the period being examined (Plotnikov and Barkova, 2007; Uyeda et. al., 2009; Muella et al., 2009).

DISCUSSION

Hines'(1960) classic work indicated that acoustic gravity waves generated in the lower atmosphere propagate upwards and are amplified as they rise due to lower atmospheric density with height. Typically during a typhoon these disturbances can be seen as travelling ionospheric disturbances (TIDs). Such disturbances are particularly evident when a typhoon is near coastal regions (Xiao et al., 2007). It is reasonable to think that 2DPCA applied in this paper was able to identify TIDs associated with Typhoon Nakri. Dhaka et al (2003) investigated intense gravity wave activities in the upper troposphere and lower stratosphere during typhoon 9426. Chun and Kim (2006) proved gravity waves can be generated by a typhoon (Typhoon Rusa), which passed through the Korean Peninsula in 2002. While in this present paper examination of typhoon-driven TEC anomalies takes place at the height of Typhoon Nakri, Kim and Chun (2011) showed that the momentum flux of typhoon generated gravity waves is greatest during the development of a typhoon and in fact this helps the typhoon develop by reducing vertical wind shear. This could suggest a good time window for a future examination of typhoon driven TEC anomalies due to gravity waves.

There is a coupling process within the troposphere-upper atmosphere – ionosphere (Pulinets, 2004). Two previous works have shown such coupling processes through earthquake-generated-gravity waves to cause TEC anomalies (Lin, 2011a; Liu et al. 2011). Liu et al (2011) was able to identify TEC anomalies caused by acoustic gravity waves resulting from the March 11 2011 great Tohoku earthquake and tsunami. 2DPCA also appeared able to detect TEC anomalies associated with China's Wenchuan earthquake due to gravity waves (Lin 2011a).

It is interesting that 2DPCA can potentially detect typhoon-driven TEC anomalies, which have in the past been detected by deviations from predetermined mean or median values for TEC. 2DPCA gives a pure mathematical basis to the detection of TEC anomalies and can describe the spatial distribution of anomalies, which may be useful in characterizing the cause of observed TEC anomalies.

There are many potential causes of ionospheric TEC anomalies besides gravity waves resulting from lower atmospheric forcings such as typhoons and earthquakes. These include internal ionospheric features, radio waves from the lower atmosphere, cosmic rays and geomagnetic storms (Lin 2010 a, b, 2011 a, b). In addition, long term variance in TEC must also be considered when applying 2DPCA. Previous studies using 2DPCA have shown that the results are not affected by long term variance (Lin, 2010b). For example, Lin (2011b) used NLPCA to examine both ionospheric TEC anomalies before the May 12 2008 Wenchuan earthquake in China and those of an earthquake-free day when a known geomagnetic storm was taking place. The magnitude of large principal eigenvalues returned (>0.5 in a normalized set) (Lin, 2010b) were relatively small for the geomagnetic storm day compared with those given for the earthquake. It seems that 2DPCA was definitely able to detect TEC anomalies due to gravity waves caused by the typhoon in this work.

Finally, another interesting finding from this study is that the approximate position of the typhoon's eye may be detectable using 2DPCA. This should be possible if the GIM can be divided into fine enough maps with adequate spatial-resolution of TEC data, such as that supplied by Japan's GEONET network system and IGSGPS tracking network, CMONOC GPS tracking network, and Shanghai GPS tracking networks.

Copyright © 2016

Leena and Luna International, Chikusei, Japan.
(株) リナアンドルナインターナショナル, 筑西市,日本
ISSN: 2186-8476, ISSN: 2186-8468 Print
www.ajsc. leena-luna.co.jp

CONCLUSION

In this study, 2DPCA is used to detect and determine the spatial distribution of a TEC anomaly, which was akin to an ionospheric tsunami that accompanied Typhoon Nakri on May 29, 2008. Analysis is conducted for the time period 12:00 to 14:00 UT on 29 May 2008. At 150-200 km the anomaly is intense and highly localized; with height, the anomaly remains intense at the same localized region but is more widespread around that point. It is assumed the anomaly relates to travelling ionospheric disturbance created by the typhoon due to acoustic gravity waves.

The results show that 2DPCA identified TEC anomalies almost above the eye of Typhoon Nakri and to a lesser extent in the surrounding typhoon zone. These findings indicate 2DPCA shows promise in finding the approximate position of a Typhoon's center if the GIM can be divided into fine enough maps with adequate spatial-resolution of TEC data.

ACKNOWLEDGEMENT

The author is grateful to Dr. J. Y. Liu and Dr C.C. Hsiao of the Institute of Space Science, Dr Louis (L.Y.) Tsai of the Graduate Institute of Applied Geology, and Dr H.W. Chen of the Institute of Geophysics, National Central University for their useful references and data support. Special gratitude is extended to the author's German professors, Dr. Jürgen Fertig and Andreas Weller of the Institute of Geophysics, Technische Universität Clausthal for my training in Germany. Finally, I'd like to thank Dan Flynn of www.planetediting.com for the English editing.

REFERENCES

[1]. Bishop, R.L., & Straus,P. R. (2006). Characterizing Ionospheric Variations in the Vicinity of Hurricanes and Typhoons Using GPS Occultation Measurements, AGU Fall Meeting (San Francisco, Dec. 11–15, 2006); EOS Transactions, *American Geophysical Union, Vol. 87*(52), Suppl. (Dec. 26, 2006), Report No. SA33B-0276.

[2]. Chun, H.Y., & Kim, S. Y. (2006).A numerical study on gravity waves generated by Typhoon Rusa. *Geophysical Research Abstracts*, *Vol. 8*, 06606, SRef-ID: 1607-7962/gra/EGU06-A-06606

[3]. Dhaka, S. K., Takahashi, M., Shibagaki, Y., Yamanaka, M. D., & Fukao, S. (2003).Gravity wave generation in the lower stratosphere due to passage of the typhoon 9426 (Orchid) observed by the MU radar at Shigaraki (34.85°N, 136.10°E), *J. Geophys. Res.*, *108*(D19), 4595, DOI:10.1029/2003JD003489.

[4]. Elsner, J.B., & Kavlakov, S. P. (2001). Hurricane intensity changes associated with geomagnetic variation. Atmospheric Science Letters (2001). doi:10.1006/asle.2001.0040

[5]. Hamilton, D. C., Gloeckler, G., Ipavich, F. M., Studemann, W., Wilken, B., & Kremser, G. (1986). Ring current development during the great geomagnetic storm of February. *J. Geophys. Res. 93*, 14343.

[6]. Hines, C.O. (1960). Internal Atmospheric Gravity Waves at Ionospheric Heights, Can. J. Phys, Vol. 38, No. 11 : pp. 1441-1481DOI: 10.1139/p60-150

Copyright © 2016

[7]. Huang, Y.N., Cheng, K., & Chen, S.W. (1985). On the detection of acoustic-gravity waves generated by typhoon by use of real time HF Doppler frequency shift sounding system, *Radio Sci., 20*(4), 897–906, doi: 10.1029/RS020i004p00897

[8]. Jin, S., W. Zhu and E. Afraimovich. (2010). Co-seismic ionospheric and deformation signals on the 2008 magnitude 8.0 Wenchuan Earthquake from GPS observations. *International Journal of Remote Sensing. Vol. 31*(13), p. 3535 - 3543.

[9]. Kazimirovsky, E. (2002). Coupling from below as a source of ionospheric variability: a review. *Annals of Geophysics, Vol. 45*(1), February 2002.

[10]. Kazimirovsky, E., Herraiz M., & De La Morena, B. A. (2003). Effects on the Ionosphere Due to Phenomena Occurring Below it. Effects on the Ionosphere Due to Phenomena Occurring Below it. *Surveys in Geophysics, Vol.24*(2), 139-184, DOI: 10.1023/A: 1023206426746.

[11]. Kim, S. Y., & Chun, H. Y. (2011). Impact of typhoon-generated gravity waves in the typhoon development. *Geophysical Research Letters, Vol. 38*, L01806, doi:10.1029/2010GL045719

[12]. Lee, J. K., Kamalabadi, F., & Makela, J. J. (2008). Three-dimensional tomography of ionospheric variability using a dense GPS receiver array, *Radio Sci., 43*, RS3001, doi:10.1029/2007RS003716.

[13]. Lin, J.W. (2010a). Two-Dimensional Ionospheric Total Electron Content Map (TEC) Seismo-Ionospheric Anomalies through Image Processing using Principal Component Analysis. *Advances in Space Research, 45*, 1301-1310.

[14]. Lin, J.W. (2010b). Ionospheric Total Electron Content (TEC) Anomalies Associated with Earthquakes through Karhunen-Loéve Transform (KLT). *Terr. Atmos. Ocean. Sci., Vol.21*(2), 253-265.

[15]. Lin, J.W, (2011a). Use of principal component analysis in the identification of the spatial pattern of an ionospheric total electron content anomalies after China's May 12, 2008, M=7.9 Wenchuan earthquake. Advances in Space Research, 47 1983–1989. DOI:10.1016/j.asr.2011.01.013.

[16]. Lin, J.W, (2011b). Potential Reasons for Ionospheric Anomalies Immediately Prior to China's Wenchuan Earthquake on 12 May 2008 Detected by Nonlinear Principal Component Analysis. International Journal of Applied Earth Observations and Geoinformation. 10.1016/j.jag.2011.09.011, (in press).

[17]. Liu, J. Y. et al., (2010). Coseismic ionospheric disturbances triggered by the Chi-Chi earthquake, *J. Geophys. Res., 115*, A08303, doi: 10.1029/2009JA014943

[18]. Liu, J. Y., Chen, C. H., Lin, C. H., Tsai, H. F., Chen, C. H., & Kamogawa, M. (2011). Ionospheric disturbances triggered by the 11 March 2011 M9.0 Tohoku earthquake, *J. Geophys. Res., 116*, A06319, doi: 10.1029/2011JA016761.

[19]. Liu, Y. M., Wang, J.S., Xiao, Z., & Suo, Y.C. (2006a). A possible mechanism of typhoon effects on the ionospheric F2 layer (in Chinese). *Chin J Space Sci, 2006, 26*: 92–97

[20]. Liu, Y M., Wang, J.S., & Suo, Y.C. (2006b). Effects of typhoon on the ionosphere. *Adv Geosci, 2006, 29*: 351–360

Copyright © 2016

Leena and Luna International, Chikusei, Japan.
(株) リナアンドルナインターナショナル, 筑西市,日本
ISSN: 2186-8476, ISSN: 2186-8468 Print
www.ajsc. leena-luna.co.jp

[21]. Londoño, E. G., López, L. C., & Kazmierczak, T. S. (2005v Using the Karhunen Loève Transform to suppress ground roll in seismic data. *Earth Sci. Res. J. Vol.9*(2), 139-147.

[22]. Mao, T., Wang., J.S., Yang, G.L., Yu, T., Ping, J.S., & Suo, Y. C. (2009). Effects of typhoon Matsa on ionospheric TEC. *Chinese Science Bulletin*, *55*(8), 712-717, DOI: 10.1007/s11434-009-0472-0

[23]. Muella, M.T.A.H., Paula, E.R.de, Kantor, I.J., Rezende, L.F.C., & Smorigo, P.F. (2009). Occurrence and zonal drifts of small-scale ionospheric irregularities over an equatorial station during solar maximum – Magnetic quiet and disturbed conditions. *Advances in Space Research*. *43*(12), p.1957-1973

[24]. Mukherjee, G.K. (1999). Storm-associated Variations of [OI] 630.0 nm Emissions from Low Latitudes. Terrestrial. *Atmospheric. Oceanic. Sciences, Vol.10*(1), 265-276.

[25]. Ping, J. Y. et al., (2002).Regional ionosphere map over Japanese Islands. *Earth Plants Space, 54,* 13-16.

[26]. Plotnikov, I. Ya., & Barkova, E.S. (2007). Advances in space research nonlinear dependence of Dst and AE indices on the electric field of magnetic clouds. *Advances in Space Research. Vol.40* (12), p.1858-1862.

[27]. Pulinets, S. A. (2004). Ionospheric Precursors of Earthquakes; Recent Advances in Theory and Practical Applications. Terrestrial. Atmospheric. *Oceanic. Sciences, Vol. 15*, No.3, 413-435.

[28]. Sanguansat, P. (2012). Principal Component Analysis, Published by InTech, Janeza Trdine 9, 51000 Rijeka, Croatia. 300pp

[29]. Shen, C. S. (1982). The correlations between the typhoon and the foF2 of ionosphere (in Chinese). *Chin J Space Sci, 2:* 335–340.

[30]. Sun, L., Wan, W., Ding, F. & Mao, T. (2007). Gravity wave propagation in the realistic atmosphere based on a three-dimensional transfer function model. Ann. *Geophys.*, *25*, 1979–1986, 2007

[31]. Xiao, Z., Xiao, S. G., Hao, Y. Q., & Zhang, D. H. (2007). Morphological features of ionospheric response to typhoon. *Journal of Geophysical Research, Vol. 112,* A04304, DOI:10.1029/2006JA011671

[32]. Xu, G., Wan, W., She, C., & Du, L. (2008). The relationship between ionospheric total electron content (TEC) over East Asia and the tropospheric circulation around the Qinghai-Tibet Plateau obtained with a partial correlation method. *Advances in Space Research*, *42*(1), 1 July 2008, p. 219-223.

[33]. Uyeda, S., Kamogawa, M., & Tanaka, H. (2009). Analysis of electrical activity and seismicity in the natural time domain for the volcanic-seismic swarm activity in 2000 in the Izu island region, Japan. *Journal of Geophysical Research .114*, B02310, 2009.

[34]. Vasilescu, M.A.O., & Terzopoulos, D. (2007). Multilinear (Tensor) Image Synthesis, Analysis, and Recognition. *IEEE Signal Processing Magazine, 119*, pp.6

[35]. Zhang, L., Lukac, R., Wu. X., & Zhang, D. (2009). PCA-Based Spatially Adaptive Denoising of CFA Images for Single-Sensor Digital Cameras. *IEEE Transactions on Image Processing*, *Vol. 18*(4), p797-812.

Copyright © 2016